DALTON

Pentafluorophenylphosphine complexes of platinum(II); crystal structure of *trans*-$[PtCl_2(PEt_3)\{PPh_2(C_6F_5)\}]$

Malcolm J. Atherton,[a] John Fawcett,[b] John H. Holloway,[b] Eric G. Hope,[b] David R. Russell[b] and Graham C. Saunders*[,b]

[a] *BNFL Fluorochemicals Ltd., Springfields, Salwick, Preston, UK PR4 0XJ*
[b] *Department of Chemistry, University of Leicester, Leicester, UK LE1 7RH*

The reactions between the pentafluorophenylphosphines $PPh_x(C_6F_5)_{3-x}$ (x = 0–2) and the dimeric platinum(II) species $[\{Pt(PEt_3)Cl(\mu\text{-}Cl)\}_2]$ yielded the complexes *trans*-$[PtCl_2(PEt_3)\{PPh_x(C_6F_5)_{3-x}\}]$ (x = 0 **1**, 1 **2** or 2 **3**). The molecular structure of complex **3** has been determined by single-crystal X-ray crystallography, it crystallizes in the triclinic space group $P\bar{1}$ with Z = 4 with two independent molecules in the asymmetric unit, a = 12.067(2), b = 14.131(1), c = 16.393(2) Å, α = 76.92(1), β = 79.08(1), γ = 89.40(1)°. Variable-temperature ^{19}F NMR spectroscopic studies, performed at 282.41 MHz, were carried out and showed that there is hindered rotation about the P–C_6F_5 bonds of complex **1**, which was frozen out at 197 K. There was no evidence of hindered rotation about the P–C bonds of complexes **2** and **3** down to 184 K.

As part of our continuing study into the effects that the presence of fluorine at strategic sites in ligands can bestow upon transition-metal complexes, we have investigated rhodium and iridium complexes of $P(C_6F_5)_3$,[1,2] $PPh(C_6F_5)_2$[1] and $PPh_2(C_6F_5)$.[1] We have found that, for bis(phosphine) complexes of rhodium(I), the ligand $P(C_6F_5)_3$ gives rise to dramatically different structural and spectroscopic properties from those of the ligands $PPh(C_6F_5)_2$ and $PPh_2(C_6F_5)$. In particular, $[\{RhCl[P(C_6F_5)_3]_2\}_n]$ is polymeric whereas $[\{RhCl[PPh_x(C_6F_5)_{3-x}]_2\}_2]$ (x = 1 or 2) are dimeric, and the absolute values of ^1J(RhP) for *trans*-$[RhCl(CO)\{PPh_x(C_6F_5)_{3-x}\}_2]$ (x = 1 or 2) are similar, whilst that for *trans*-$[RhCl(CO)\{P(C_6F_5)_3\}_2]$ is considerably larger. We have extended our study to platinum(II) species of the form $[PtCl_2(PEt_3)L]$ (L = fluorinated phosphines) and we report here the synthesis and characterization of these complexes and the structure of *trans*-$[PtCl_2(PEt_3)\{PPh_2(C_6F_5)\}]$.

Results and Discussion

The reactions between the pentafluorophenylphosphines $PPh_x(C_6F_5)_{3-x}$ (x = 0–2) and the dimeric platinum(II) species $[\{PtCl(\mu\text{-}Cl)(PEt_3)\}_2]$ in refluxing acetone yielded the complexes *trans*-$[PtCl_2(PEt_3)\{PPh_x(C_6F_5)_{3-x}\}]$ (x = 0 **1**, 1 **2** or 2 **3**). The complexes were characterized by elemental analyses, mass spectroscopy, ^{1}H, ^{19}F and ^{31}P NMR and IR spectroscopies (Table 1). The assignments of the phosphorus resonances were made by comparison of the ^{31}P and ^{31}P-{^{1}H} NMR spectra. The magnitude of the platinum–phosphorus coupling constant, ^1J(PtP), and for the complexes **1** and **2**, the magnitude of the phosphorus–phosphorus coupling constant, ^2J(PP), confirm that each complex possesses mutually *trans* phosphine ligands. This is further confirmed by the molecular structure of complex **3** (Fig. 1), which was determined by single-crystal X-ray diffraction. The ^{31}P-{^{1}H} NMR spectrum of **3** is second order exhibiting two signals at δ_P 14.4 and 14.3, each with platinum satellites. A simulation of this spectrum give values of δ_P of 13.9 and 14.8 with absolute values for ^1J(PtP) of 2470 and 2615 Hz respectively, and an absolute value for ^2J(PP) of 469 Hz. The assignment of the two resonances is difficult because of the very second-order nature of the spectrum. However, a careful inspection of the high frequency ^{195}Pt satellites in the undecoupled ^{31}P NMR spectrum allows assignment of the higher-frequency resonance (δ_P 14.8) to the PEt_3 ligand, in line with that observed for complexes **1** and **2**. The values of δ_P for the fluorine-containing phosphine resonances of complexes **1**–**3** are *ca.* 50 ppm to higher frequency than those for the free ligands. The magnitude of $^1J[Pt\text{–}PPh_x(C_6F_5)_{3-x}]$ increases in the order **1** < **2** < **3**, which is consistent with previous observations and is accounted for by the expected increase in the C–P–C angles, and thus lower s-character of the Pt–P bond, as C_6H_5 is replaced by C_6F_5.[3,4] (This series differs significantly from the sequence of the absolute values of the rhodium–phosphorus coupling constants, ^1J(RhP), for the complexes *trans*-$[RhCl(CO)\{PPh_x(C_6F_5)_{3-x}\}]$, in which ^1J(RhP) for the complexes x = 1 and 2 are similar and that for x = 0 is considerably greater.[1]) The value of δ and the magnitude of ^1J(PtP) for the PEt_3 ligand follow the order **1** > **2** > **3**. The magnitude of ^2J(PP) follows the same order.

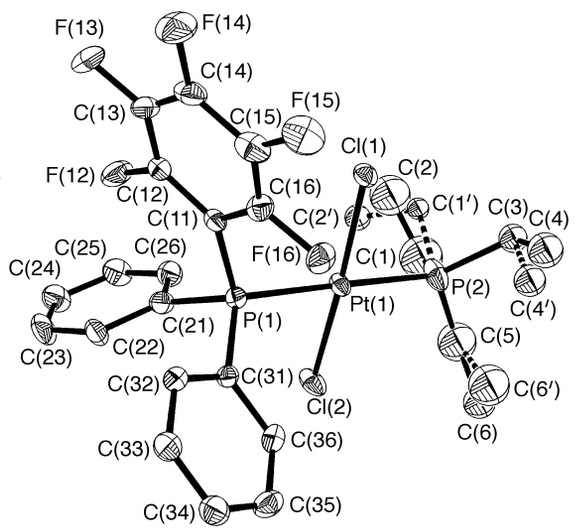

Fig. 1 Molecular structure of one of the independent molecules of *trans*-$[PtCl_2(PEt_3)\{PPh_2(C_6F_5)\}]$ **3**. Displacement ellipsoids are shown at the 30% probability level. The hydrogen atoms are omitted for clarity

The structure of complex **3** possesses two independent molecules in the asymmetric unit. Selected bond lengths, bond angles and torsion angles are given in Table 2. The *trans* geometry of the complex is confirmed by the crystal structure with P–Pt–P angles of *ca.* 178° and Cl–Pt–Cl angles of *ca.* 174°. The P–Pt–Cl angles lie in the range 88.25(9)–92.93(7)°. The two independent molecules within the asymmetric unit possess

Table 1 Analytical, mass spectral and NMR spectroscopic data for compounds **1**–**3**

Compound	Analysis (%)[a] and *m*/z[b]	NMR Spectroscopy[c]
1[d]	C, 29.6 (31.5); H, 2.0 (1.65) 915 (M^+), 880 ($[M - Cl]^+$), 843 ($[M - 2Cl - 2H]^+$)	^{1}H: 1.97 (6 H, m, CH_2), 1.20 [9 H, dt, ^3J(PH) 17.5, ^3J(HH) 7.6, CH_3] ^{19}F: −126.18 (6 F, br m, *o*), −145.41 (3 F, unresolved t, *p*), −159.29 (6 F, m, *m*) ^{19}F(197 K): −120.65 (2 F, m, *o*), −127.97 (2 F, m, *o*), −130.70 (2 F, m, *o*), −142.14 (2 F, m, *p*), −144.30 (1 F, m, *p*), −158.29 (2 F, vt, *J* 23.2, *m*), −158.77 (2 F, vt, *J* 20.7, *m*), −159.50 (2 F, m, *m*) ^{31}P-{^{1}H}: 18.8 [d, ^2J(PP) 532, ^1J(PtP) 2918, PEt_3], −18.1 [d, ^2J(PP) 532, ^1J(PtP) 2255, $P(C_6F_5)_3$]
2	C, 35.1 (34.9); H, 2.4 (2.4) 826 ($[M + H]^+$), 791 ($[M - Cl + H]^+$), 755 ($[M - 2Cl]^+$)	^{1}H: 7.90 (2 H, m, PPh), 7.52 (1 H, m, *p*), 7.45 (2 H, m, PPh), 1.98 (6 H, m, CH_2), 1.22 [9 H, dt, ^3J(PH) 17.0, ^3J(HH), 7.7, CH_3] ^{19}F: −124.88 [4 F, dm, $^3J(F_oF_m)$ 19.3, *o*], −147.13 [2 F, tm, $^3J(F_mF_p)$ 20.8, *p*], −159.95 (4 F, m, *m*) ^{31}P-{^{1}H}: 16.7 [d, ^2J(PP) 508, ^1J(PtP) 2792, PEt_3], 0.8 [d, ^2J(PP) 508, ^1J(PtP) 2344, $PPh(C_6F_5)_2$]
3	C, 39.4 (39.15); H, 3.5 (3.4) 736 ($[M + H]^+$), 701 ($[M - Cl + H]^+$), 665 ($[M - 2Cl]^+$)	^{1}H: 7.97 (4 H, m, PPh_2), 7.43 (6 H, m, PPh_2), 2.01 (6 H, m, CH_2), 1.25 [9 H, dt, ^3J(PH) 17.3, ^3J(HH) 7.4, CH_3] ^{19}F: −124.80 [2 F, dm, $^3J(F_oF_m)$ 20.8, *o*], −149.39 [1 F, tm, $^3J(F_mF_p)$ 20.7, *p*], −161.05 [2 F, ddm, $^3J(F_mF_p) \approx {}^3J(F_mF_o)$ 20.9, *m*] ^{31}P-{^{1}H} ABX pattern, 14.8 [^2J(PP) 469, ^1J(PtP) 2615, PEt_3], 13.9 [^2J(PP) 469, ^1J(PtP) 2470, $PPh_2(C_6F_5)$][e]

[a] Required values are given in parentheses. [b] FAB mass spectra in *m*-nitrobenzyl alcohol matrix. [c] Recorded in $CDCl_3$ at 298 K, unless stated otherwise. Data given as: chemical shift (δ) [relative intensity, multiplicity (*J* in Hz), assignment], d = doublet, t = triplet, vt = virtual triplet, m = multiplet. [d] Samples of **1** were contaminated with small amounts of $[\{PtCl(\mu\text{-}Cl)(PEt_3)\}_2]$, repeated recrystallizations failed to give satisfactory analysis. [e] Values obtained from simulation.

Table 2 Selected bond lengths (Å), angles (°) and torsion angles (°) with estimated standard deviations (e.s.d.s) in parentheses for *trans*-$[PtCl_2(PEt_3)\{PPh_2(C_6F_5)\}]$ **3**

Pt(1)–Cl(1)	2.305(2)	Pt(2)–Cl(1a)	2.303(2)
Pt(1)–Cl(2)	2.307(2)	Pt(2)–Cl(2a)	2.318(2)
Pt(1)–P(1)	2.318(2)	Pt(2)–P(1a)	2.322(2)
Pt(1)–P(2)	2.299(2)	Pt(2)–P(2a)	2.300(2)
P(1)–C(11)	1.852(8)	P(1a)–C(11a)	1.849(9)
P(1)–C(21)	1.802(9)	P(1a)–C(21a)	1.809(9)
P(1)–C(31)	1.814(8)	P(1a)–C(31a)	1.813(8)
Cl(1)–Pt(1)–Cl(2)	174.03(9)	Cl(1a)–Pt(2)–Cl(2a)	173.45(9)
P(1)–Pt(1)–Cl(1)	92.93(7)	P(1a)–Pt(2)–Cl(1a)	91.58(7)
P(1)–Pt(1)–Cl(2)	88.61(8)	P(1a)–Pt(2)–Cl(2a)	89.43(7)
P(2)–Pt(1)–Cl(1)	88.25(9)	P(2a)–Pt(2)–Cl(1a)	88.31(8)
P(2)–Pt(1)–Cl(2)	90.21(9)	P(2a)–Pt(2)–Cl(2a)	90.40(8)
P(1)–Pt(1)–P(2)	178.82(9)	P(1a)–Pt(2)–P(2a)	117.52(9)
Pt(1)–P(1)–C(11)	113.8(2)	Pt(2)–P(1a)–C(11a)	112.8(2)
Pt(1)–P(1)–C(21)	112.9(3)	Pt(2)–P(1a)–C(21a)	111.0(3)
Pt(1)–P(1)–C(31)	117.6(3)	Pt(2)–P(1a)–C(31a)	118.4(3)
C(11)–P(1)–C(21)	105.3(4)	C(11a)–P(1a)–C(21a)	105.7(4)
C(11)–P(1)–C(31)	100.2(4)	C(11a)–P(1a)–C(31a)	100.9(4)
C(21)–P(1)–C(31)	105.7(4)	C(21a)–P(1a)–C(31a)	107.0(4)
C(11)–P(1)–Pt(1)–Cl(1)	−2.6	C(11a)–P(1a)–Pt(2)–Cl(1a)	8.1
Pt(1)–P(1)–C(11)–C(12)	111.1	Pt(2)–P(1a)–C(11a)–C(12a)	74.1
Pt(1)–P(1)–C(11)–C(16)	−67.1	Pt(2)–P(1a)–C(11a)–C(16a)	−104.2
Pt(1)–P(1)–C(21)–C(22)	158.4	Pt(2)–P(1a)–C(21a)–C(22a)	−165.6
Pt(1)–P(1)–C(21)–C(26)	−24.0	Pt(2)–P(1a)–C(21a)–C(26a)	19.0
Pt(1)–P(1)–C(31)–C(32)	156.5	Pt(2)–P(1a)–C(31a)–C(32a)	15.5
Pt(1)–P(1)–C(31)–C(36)	−22.2	Pt(2)–P(1a)–C(31a)–C(36a)	−160.0

$Pt–PPh_2(C_6F_5)$ bond lengths which are identical within experimental error. The $Pt–PEt_3$ bond lengths in the two unique molecules are also identical, and they are shorter than the $Pt–PPh_2(C_6F_5)$ bonds by *ca.* 0.02 Å. In both molecules the planes defined by the $Pt–PPh_2(C_6F_5)$ and $P–C_6F_5$ bonds are almost coplanar with the PtP_2Cl_2 plane [*i.e.* the Cl(1)–Pt–P–C_6F_5 torsion angles are close to 0°]. Both molecules show a similar disposition of the phenyl rings about the Pt–P axis. The planes defined by the C_6H_5 rings are twisted by *ca.* 20° from parallel with the Pt–P bond giving the Pt–P–C–C torsion angles close to 20 and 160° for each ring. The plane defined by the C_6F_5 ring is twisted away from perpendicular to the Pt–P bond at *ca.* 20° such that the absolute Pt–P–C–C torsion angles are *ca.* 70 and 110°. The P–C bond lengths of the $PPh_2(C_6F_5)$ ligand are the same within experimental error. Both Pt–P–C_6F_5 angles are *ca.* 113° with each unique molecule possessing one smaller Pt–P–C_6H_5 angle at *ca.* 112° and one larger angle of *ca.* 118°. These values may be compared to those in the platinum(II) complex *trans*-$[PtMe\{PPh_2(C_6F_5)\}(OC_6F_4PPh_2\text{-}2)]$,[5] in which the P–$C_6F_5$ bond is significantly longer than the P–C_6H_5 bonds and the Pt–P–C_6F_5 angle of 109.7(3)° is considerably smaller than the Pt–P–C_6H_5 angles of 114.4(2) and 116.8(2)°. The C–P–C angles of the $PPh_2(C_6F_5)$ ligand in **3** lie in the range 100.2(4)–107.0(4)°. The bond lengths and angles of the C_6F_5 rings in the structure of **3** are similar to those in *trans*-$[PtMe\{PPh_2(C_6F_5)\}(OC_6F_4PPh_2\text{-}2)]$.

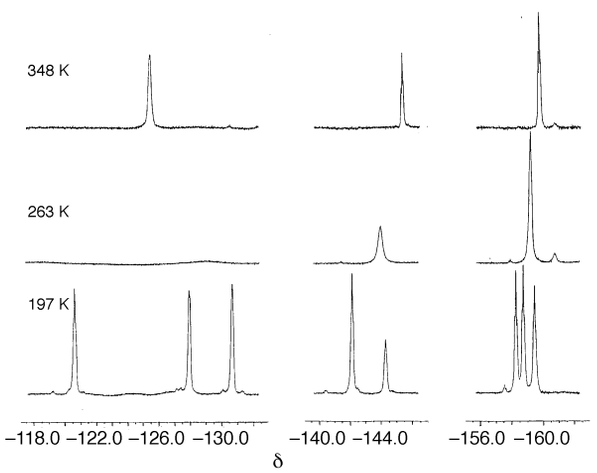

Fig. 2 Variable-temperature ^{19}F NMR spectra of *trans*-$[PtCl_2(PEt_3)\{P(C_6F_5)_3\}]$ **1** in $CDCl_3$ at 282.41 MHz

The ^{19}F NMR spectrum of complex **1**, recorded at 282.41 MHz, in $CDCl_3$ at 298 K shows three resonances at δ_F −126.18, −145.41 and −159.29 assigned to the *o*-, *p*- and *m*-fluorine atoms respectively. The resonance assigned to the *o*-fluorines is broad, indicative of a fluxional process. At 348 K the *o*-fluorine resonance is considerably sharper. Upon cooling from 298 K the three resonances broaden significantly and at 197 K there are eight sharp resonances (Fig. 2, Table 1). The presence of only two resonances at δ −140.0 to −145.0, with intensities in a ratio of 2:1, assigned to the *p*-fluorines is consistent with two equivalent and one unique C_6F_5 ring (Fig. 3, F_h and F_c). The presence of three resonances at δ −118.0 to −132.0, with equal intensities, assigned to the *ortho* fluorine atoms and three reson-

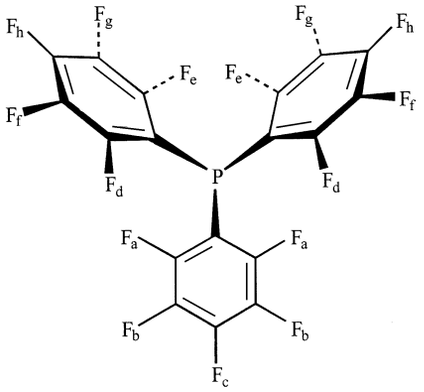

Fig. 3 Diagrammatic representation of the arrangement of the C_6F_5 rings of $P(C_6F_5)_3$ in *trans*-$[PtCl_2(PEt_3)\{P(C_6F_5)_3\}]$ **1** at the low-temperature limit

ances at δ −156.0 to −160.0, with equal intensities, assigned to the *meta* fluorine atoms is consistent with the two *ortho* fluorine atoms on the unique C_6F_5 ring being equivalent (F_a), the two *meta* fluorine atoms on the unique C_6F_5 ring being equivalent (F_b), and the two *ortho* fluorine atoms on each equivalent ring being non-equivalent (F_d and F_e) and the two *meta* fluorine atoms on each equivalent ring being non-equivalent (F_f and F_g). These data are similar to those of the low-temperature ^{19}F NMR spectra of *trans*-$[PtCl_2(PPh_3)\{P(C_6F_5)_3\}]$ and *trans*-$[PtBr_2(PPhMe_2)\{P(C_6F_5)_3\}]$[3] and are consistent with hindered rotation about the P–C_6F_5 bonds of the two equivalent C_6F_5 rings. It is not essential to infer hindered rotation about the unique P–C_6F_5 bond to explain these data, but investigations into the molecular dynamics of *trans*-platinum(II) bis(phosphine) complexes, in particular *trans*-$[PtCl(Ph)(PMePh_2)\{P(C_6F_5)_3\}]$,[3] indicate that there is hindered rotation about all the P–C bonds of the $P(C_6F_5)_3$ ligand in this case. It could well be that this is also the case for complex **1**. It seems likely that, at the low-temperature limit, the $P(C_6F_5)_3$ ligand adopts a conformation where the plane of the unique C_6F_5 ring lies almost perpendicular to the Pt–P bond, such that the two Pt–P–C–C torsion angles are close to 90 and −90°, and the pair of identical C_6F_5 rings adopt conformations twisted from parallel to the Pt–P bond by the same amount such that the absolute values of the Pt–P–C–C torsion angles for each ring are very different. Such a conformation is, however, not consistent with conformations adopted by the $P(C_6F_5)_3$ ligands of the four-co-ordinate, bis(phosphine) complexes *trans*-$[IrBr(CO)\{P(C_6F_5)_3\}]$,[2] *trans*-$[PtX_2\{P(C_6F_5)_3\}_2]$ (X = Cl[6] or I[7]) and *trans*-$[PdCl_2\{P(C_6F_5)_3\}_2]$[8] in the solid state. In these complexes the $P(C_6F_5)_3$ ligands adopt conformations in which one C_6F_5 ring is parallel to the Pt–P bond (absolute Pt–P–C–C torsion angles of 0–13 and 172–180°) and two C_6F_5 rings lie twisted by *ca.* 30° from perpendicular to the Pt–P bond (absolute Pt–P–C–C torsion angles of 51–67 and 105–120°). The compounds *trans*-$[PtX_2\{P(C_6F_5)_3\}_2]$ (X = Cl or I)[3] show similar fluxional behaviour to *trans*-$[PtCl_2\{P(C_6F_5)_3\}L]$ (L = PMe_3 or PPh_3)[3] and *trans*-$[PtBr_2(PPhMe_2)\{P(C_6F_5)_3\}]$[3] and thus it appears that, in four-co-ordinate platinum(II) complexes, the $P(C_6F_5)_3$ ligand adopts a different conformation in solution to that in the solid state. A variable-temperature ^{31}P-{^1H} NMR spectroscopic study (121.50 MHz) of complex **1** in CD_2Cl_2 shows no fluxional processes, with only a slight broadening of the signals at 184 K. Thus, there is no evidence to suggest hindered rotation about the Pt–P bonds in complex **1** under the conditions of the study.

Complexes **2** and **3** do not show fluxional behaviour similar to that of **1**. The ^{19}F (282.41 MHz) and ^1H (300.14 MHz) NMR spectra show only sharp resonances at 298 K, and at 184 K in CD_2Cl_2 no significant broadening of either the ^{19}F or ^1H spectroscopic resonances is observed. The replacement of one C_6F_5 group in $P(C_6F_5)_3$ by a phenyl ring is evidently sufficient to allow essentially unhindered rotation about all the P–C bonds.

In summary, the complexes *trans*-$[PtCl_2(PEt_3)\{PPh_x(C_6F_5)_{3-x}\}]$ have been synthesized and their molecular dynamics studied by variable-temperature ^1H, ^{19}F and ^{31}P NMR spectroscopy. Our investigation shows that the electronic properties of the ligands in these complexes vary regularly, unlike those in the system *trans*-$[RhCl(CO)\{PPh_x(C_6F_5)_{3-x}\}]$,[1] but that rotation about the P–C bonds of $P(C_6F_5)_3$ in complex **1** is considerably more hindered than that of $PPh(C_6F_5)_2$ and $PPh_2(C_6F_5)$ in complexes **2** and **3** respectively.

Experimental

Physical measurements

The ^1H, ^{19}F and ^{31}P NMR spectra were recorded on a Bruker AM300 spectrometer at 300.14, 282.41 and 121.50 MHz respectively, ^1H referenced internally using the residual protio solvent resonance relative to tetramethylsilane (δ 0), ^{19}F externally to $CFCl_3$ (δ 0) and ^{31}P externally to 85% H_3PO_4 (δ 0). Infrared spectra were recorded as Nujol mulls between KBr plates on a Digilab FTS40 Fourier-transform spectrometer. Elemental analyses were performed by Butterworth Laboratories Ltd. and FAB mass spectra were recorded on a Kratos Concept 1H mass spectrometer.

Materials

The phosphines $P(C_6F_5)_3$, $PPh(C_6F_5)_2$ and $PPh_2(C_6F_5)$ (Fluorochem) were used as supplied. The platinum complex $[\{PtCl(\mu\text{-}Cl)(PEt_3)\}_2]$ was prepared as described previously.[9] Light petroleum (b.p. 40–60 °C) was used throughout.

Preparations

***trans*-$[PtCl_2(PEt_3)\{P(C_6F_5)_3\}]$ 1.** A slurry of $[\{PtCl(\mu\text{-}Cl)(PEt_3)\}_2]$ (0.24 g, 0.31 mmol) and $P(C_6F_5)_3$ (0.27 g, 0.50 mmol) in acetone (30 cm^3) was refluxed for 1 min to give a pale yellow solution. The solution was allowed to cool and filtered. The solvent was removed by rotary evaporation to give **1** as a yellow solid, which was dried *in vacuo*. Yield 0.17 g, 31%. IR: 1646m, 1520s, 1488s, 1391m, 1297m, 1264w, 1239w, 1150w, 1097s, 1038m, 1012w, 986s, 856w, 785m, 739w, 724w, 639w, 631w, 589w, 520w and 459w cm^{-1}.

***trans*-$[PtCl_2(PEt_3)\{PPh(C_6F_5)_2\}]$ 2.** A slurry of $[\{PtCl(\mu\text{-}Cl)(PEt_3)\}_2]$ (0.15 g, 0.20 mmol) and $PPh(C_6F_5)_2$ (0.17 g, 0.38 mmol) in acetone (50 cm^3) was refluxed for 5 min to give a pale yellow solution. The solution was allowed to cool, filtered and concentrated by rotary evaporation to *ca.* 10 cm^3. Addition of light petroleum (30 cm^3) afforded yellow crystals of **2**, which were washed with light petroleum and dried *in vacuo*. Yield 0.13 g, 41%. IR: 1644m, 1522s, 1488s, 1437m, 1413w, 1394m, 1312w, 1293m, 1260w, 1096s, 1040m, 979s, 849w, 772m, 744m, 724m, 704w, 688m, 633m, 588w, 524m, 513w, 487w, 476m and 451w cm^{-1}.

***trans*-$[PtCl_2(PEt_3)\{PPh_2(C_6F_5)\}]$ 3.** A slurry of $[\{PtCl(\mu\text{-}Cl)(PEt_3)\}_2]$ (0.145 g, 0.19 mmol) and $PPh_2(C_6F_5)$ (0.122 g, 0.35 mmol) in acetone (50 cm^3) was refluxed for 5 min to give a pale yellow solution. The solvent was removed by rotary evaporation to yield a yellow solid, which was recrystallized from dichloromethane. Yield 0.06 g, 21%. IR: 1645m, 1522s, 1488s, 1439w, 1412w, 1391w, 1290m, 1261w, 1085s, 1040m, 979s, 851w, 841w, 770m, 743m, 724m, 704w, 689m, 632m, 587w, 525m, 511m, 486w, 475w, 449w and 430m cm^{-1}.

Crystal-structure determination of complex 3

Crystal data and data collection parameters. $C_{24}H_{25}Cl_2F_5P_2Pt$, $M = 736.37$, triclinic, $a = 12.067(2)$, $b = 14.131(1)$, $c = 16.393(2)$ Å, $\alpha = 76.92(1)$, $\beta = 79.08(1)$ $\gamma = 89.40(1)°$, $U = 2672.0(6)$ $Å^3$ (by least-squares refinement on diffractometer

angles from 28 centred reflections, $10.0 < 2\theta < 24.6°$), T = 190(2) K, space group $P\bar{1}$, graphite-monochromated Mo-Kα radiation, $\lambda = 0.710\ 73$ Å, $Z = 4$ with two independent molecules in the asymmetric unit, $D_c = 1.831$ g cm^{-1}, $F(000) = 1424$, dimensions $0.48 \times 0.41 \times 0.21$ mm, μ(Mo-Kα) = 5.618 mm^{-1}, semiempirical absorption correction based on ψ scans, maximum and minimum transmission factors 0.95 and 0.365, Siemens P4 diffractometer, ω scans, data collection range $5.2 < 2\theta < 54.0°$, $-1 \leqslant h \leqslant 14$, $-17 \leqslant k \leqslant 17$, $-20 \leqslant l \leqslant 20$, no crystal decay was detected from periodically measured check reflections; 11 607 reflections measured, 11 395 unique (R_{int} = 0.0280). The data were corrected for Lorentz and polarization effects.

Structure solution and refinement. Structure solution by Patterson methods was carried out using the SHELXTL PC program.[10] Refinement by full-matrix least squares on F^2 was carried out using the program SHELXL 93.[11] An initial data set collected at room temperature was solved satisfactorily except that all ethyl carbon atoms had excessive anisotropic parameters indicative of disorder which could not be adequately modelled. The highest residual electron density was 1.6 e Å^{-3} lying in the bond between Pt(2) and Cl(2a), 1.3 Å from Pt(2). A second data set was collected from a new crystal at 190 K in an attempt to minimize the disorder. These data provided a molecular structure which displayed smaller, but still excessive, anisotropic displacement parameters for the ethyl groups suggesting that the disorder persists at 190 K. The final refinement allowed for disordered ethyl groups with restraints to the P–C [1.86(1) Å], C–C′ [1.46(1) Å] and P–C′ [2.80(5) Å] distances and isotropic displacement parameters. Essentially the disorder model allows two alternative sites for all 12 ethyl carbon atoms with 50% occupancy, but for three methylene carbon atoms [C(1), C(1b) and C(3b)] the alterative sites could not be resolved. All other non-hydrogen atoms were refined as anisotropic atoms. The hydrogen atoms of the disordered ethyl groups were not included in the refinement, all other hydrogen atoms were included in calculated positions (C–H = 0.96 Å) using a riding model. Final $R1 = 0.0484$ and $wR2 = 0.1083$ for 8266 observed reflections [$I > 2\sigma(I)$] and $R1 = 0.0798$ and $wR2 = 0.1221$ (all data) for the 589 parameters and 33 restraints refined with largest Δ/σ 0.012, goodness of fit = 1.043. The highest residual electron density peak from this data set is 3.25 e Å^{-3} and, as with the room temperature data, is 1.3 Å from Pt(2), approximately on the Pt(2)–Cl(2a) bond. The residual density, although obviously an artefact in the data, does not appear to arise from absorption. Empirical absorption corrections based on ψ scan data from over 40 reflections from both crystals were applied. A DIFABS-type refinement[12] was attempted on the 190 K data, but did not result in any significant reduction in this residual density, indicating that this problem was not due to absorption. An analytical absorption correction was not possible as the crystal did not have clearly defined faces. An analysis of the weighting scheme over $|F_o|$ and sin θ/λ was satisfactory.

Atomic coordinates, thermal parameters, and bond lengths and angles have been deposited at the Cambridge Crystallographic Data Centre (CCDC). See Instructions for Authors, *J. Chem. Soc., Dalton Trans.*, 1997, Issue 1. Any request to the CCDC for this material should quote the full literature citation and the reference number 186/533.

Acknowledgements

We thank K. S. Coleman for preliminary work, Dr. G. A. Griffith for assistance with the NMR spectroscopy experiments and the simulation, BNFL Fluorochemicals Ltd. (G. C. S.) and the Royal Society (E. G. H.) for support.

References

1 M. J. Atherton, K. S. Coleman, J. Fawcett, J. H. Holloway, E. G. Hope, A. Karaçar, L. A. Peck, D. R. Russell and G. C. Saunders, *J. Chem. Soc., Dalton Trans.*, 1995, 4029.
2 J. H. Holloway, E. G. Hope, D. R. Russell, G. C. Saunders and M. J. Atherton, *Polyhedron*, 1996, **15**, 173.
3 J. B. Docherty, D. S. Rycroft, D. W. A. Sharp and G. A. Webb, *J. Chem. Soc., Chem. Commun.*, 1979, 336.
4 R. Mason and D. W. Meek, *Angew. Chem., Int. Ed. Engl.*, 1978, **17**, 183.
5 S. Park, M. Pointer-Johnson and D. M. Roundhill, *Inorg. Chem.*, 1990, **29**, 2689.
6 W. P. Schaefer, D. K. Lyon, J. A. Labinger and J. E. Bercaw, *Acta Crystallogr., Sect. C*, 1992, **48**, 1582.
7 W. N. Hunter, K. W. Muir and D. W. A. Sharp, *Acta Crystallogr., Sect. C*, 1986, **42**, 1743.
8 B. Berstch-Frank and W. Frank, *Acta Crystallogr., Sect. C*, 1996, **52**, 328.
9 R. J. Goodfellow and L. M. Venanzi, *J. Chem. Soc. A*, 1965, 7533.
10 G. M. Sheldrick, SHELXTL PC, Release 4.2, Siemens Analytical X-Ray Instruments, Madison, WI, 1991.
11 G. M. Sheldrick, SHELXL 93, Program for Crystal Structure Refinement, University of Göttingen, 1993.
12 R. H. Blessing, *Acta Crystallogr., Sect. A*, 1995, **51**, 33.

Received 6*th December* 1996; *Paper* 6/08253J